Rock and Soil Mechanics

Volume 42 | Issue 5 Article 7

9-16-2021

Experimental study of unsaturated-saturated permeability characteristics of slip zone soil in deposits

Yue LI
Department of Civil and Environmental Engineering, University of Waterloo, Ontario, Canada

Wei-ya XU
Key Laboratory of Geomechanics and Embankment Engineering, Ministry of Education, Hohai University, Nanjing, Jiangsu 210098, China

Kui YI
Huaneng Lancang River Hydropower Inc., Kunming, Yunnan 650206, China

Wei-chau XIE
Department of Civil and Environmental Engineering, University of Waterloo, Ontario, Canada

See next page for additional authors

Custom Citation

LI Yue, XU Wei-ya, YI Kui, XIE Wei-chau, ZHANG Qiang, MENG Qing-xiang, . Experimental study of unsaturated-saturated permeability characteristics of slip zone soil in deposits[J]. Rock and Soil Mechanics, 2021, 42(5): 1355-1362.

Rock and Soil Mechanics 2021 42(5): 1355−1362
ISSN 1000−7598
https: //doi.org/10.16285/j.rsm.2020.6267
rocksoilmech.researchcommons.org/journal

Experimental study of unsaturated-saturated permeability characteristics of slip zone soil in deposits

LI Yue[1, 2], XU Wei-ya[1, 3], YI Kui[4], XIE Wei-chau[2], ZHANG Qiang[5], MENG Qing-xiang[1, 3]

1. Research Institute of Geotechnical Engineering, Hohai University, Nanjing, Jiangsu 210098, China
2. Department of Civil and Environmental Engineering, University of Waterloo, Ontario, Canada
3. Key Laboratory of Geomechanics and Embankment Engineering, Ministry of Education, Hohai University, Nanjing, Jiangsu 210098, China
4. Huaneng Lancang River Hydropower Inc., Kunming, Yunnan 650206, China
5. Research Institute of Geotechnical Engineering, China Institute of Water Resources and Hydropower Research, Beijing 100038, China

Abstract: There are many landslide deposits in the reservoir and bank areas of hydropower projects in southwest China. These deposits are easy to deform and fail along the existing sliding zone under hydrodynamic conditions, such as rainfall and reservoir water fluctuation. The slip soil in Dahua landslide deposits which are located at the Dahuaqiao Hydropower Plant in the Lancang river basin of southwest China, was studied as an example. The experimental study was carried out to explore the soil-water characteristic curve (SWCC) of slip soil. The permeability characteristics and the evolution in the unsaturated seepage process were analyzed, and the saturated permeability characteristics under different confining pressures and osmotic pressures were studied. The results indicated that the VG model could be used to describe the SWCC and the variation of relative permeability coefficient of Dahua slip zone soil. Through the saturated permeability test, it is found that under the same other conditions, the larger the confining pressure is, the weaker the saturated permeability of the slip soil is; while the larger the osmotic pressure is, the stronger the saturated permeability is. Furthermore, the saturated permeability characteristics of the slip zone soil manifested a strong non-Darcy flow behavior, and the relationship between permeability velocity and hydraulic gradient satisfied the Forchheimer binomial model. When the confining pressure was low, the linear term coefficient of velocity had a more significant effect on the permeability, whereas the quadratic term coefficient of velocity gradually dominated in the seepage process with the increase of confining pressure.

Keywords: slip zone soil in deposits; unsaturated-saturated permeability; soil-water characteristic curve (SWCC); non-Darcy flow; hydrodynamic-induced landslide

1 Introduction

Due to the special topographical features and geological conditions of the hydropower base in the mainstream of Lancang River in China, there are a large number of landslide deposits with soil-rock mixed structure in the reservoir and bank areas. Under the action of rainfall[1−2], reservoir water level[3], and other various hydrodynamic factors[4], these large-scale deposits produce the mutual feed mechanism between water and rock (soil)[5−6], which in turn induce hydrodynamic landslide[4] and other disasters[7]. This phenomenon has become a major hidden danger affecting the safety of engineering operations. Therefore, it is of great engineering value to study the stability of landslide deposits under the influence of hydrodynamic factors.

Under the action of hydrodynamic factors such as rainfall and fluctuation of reservoir water level, the water content, matric suction, and permeability of the soil in the landslide deposits will change. In soil science, the parameters related to soil hydrodynamic factors, such as water content, soil-water characteristic curve (SWCC), and unsaturated-saturated permeability coefficient are collectively referred to as hydrodynamic parameters[8]. The characteristics of these parameters directly affect the stability of landslides under the action of hydrodynamic factors. So far, it is still difficult to obtain the unsaturated permeability of soil through laboratory experiments. At present, scholars have developed various prediction models based on SWCC[9−10], which shows that SWCC is one of the foundations of hydrodynamic characteristics research. However, the studies of SWCC from literatures are basically aimed at soil landslides[11−12]. Compared with clay-dominated soils, the slip zone soil in landslide deposits has lower clay content and higher granular content. The maximum matric suction of slip zone soil is even lower than that of common clay, which has less effect on the shear strength of the soil. Therefore, little attention has been paid to the soil-water characteristic curve of the slip soil in landslide deposits. Up to now, the research on SWCC of the slip zone soil with soil–rock mixed structure is reported rarely.

For the saturated permeability of the slip zone soil in landslide deposits, it has been generally recognized that the non-Darcy characteristics of the seepage in the

Received: 21 August 2020 Revised: 27 December 2020
This work was supported by the Key Program of National Natural Science Foundation of China (51939004), the National Key R & D Program of China (2017YFC1501100), the National Natural Science Foundation of China (11772118) and the Key Project of China Huaneng Group Science and Technology (HNKJ18-H24).
First author: LI Yue, male, born in 1987, PhD, mainly engaged in disaster prevention and mitigation of complex geotechnical engineering disasters. E-mail: Yueh.Li@foxmail.com
Corresponding author: ZHANG Qiang. male, born in 1986, PhD, Senior engineer, mainly engaged in the research of multi-scale disaster mechanism and numerical simulation of complex geotechnical media. E-mail: zhangq@iwhr.com

soil-rock mixture[13]. Forchheimer proposed that due to a relatively high seepage velocity in the soil-rock mixture, the flow pattern has developed from laminar flow to turbulent flow[14]. But most of the studies only focus on the relationship between permeability characteristics and rock content or a particular particle size in the landslide deposits[15–18]. In fact, in addition to the influence of material composition of landslide deposits, the confining pressure, the groundwater level and the reservoir water level are also factors that cannot be ignored. The burial depth of the slip zone soil in the landslide deposits is different, and it will be affected by different confining pressures; the changes of groundwater and reservoir water level will cause the change of osmotic pressure. These two factors will undoubtedly have an impact on the permeability characteristics. However, at present, there are few studies on the permeability characteristics of the slip soil in landslide deposits under different confining pressures and osmotic pressures.

In this backdrop, the slip zone soil of Dahua landslide deposits in reservoir area of Dahuaqiao Hydropower Station in Lancang River Basin was selected as the tested material in this paper, and the soil-water characteristic curve of the slip zone soil was measured by laboratory tests. On this basis, the unsaturated permeability of slip soil was analyzed, and the saturated permeability of slip soil under different confining pressures and osmotic pressures was studied. The research results are of great significance for revealing the mechanisms of breeding, formation, development, movement, and post-disaster of the hydrodynamic landslide deposits, as well as the prevention and protection of engineering disasters.

2 Project background

Dahuaqiao Hydropower Station is located in Tu’e Township, Lanping County, Nujiang Prefecture, Yunnan Province, China (Fig.1(a)). It is the sixth stage of a development project named ‘seven-stage hydropower station in one reservoir’ on the upper reaches of the mainstream of Lancang River. The normal storage level of the reservoir is 1 477 m. The barrage is concrete gravity dam, and the maximum dam height is 107 m.

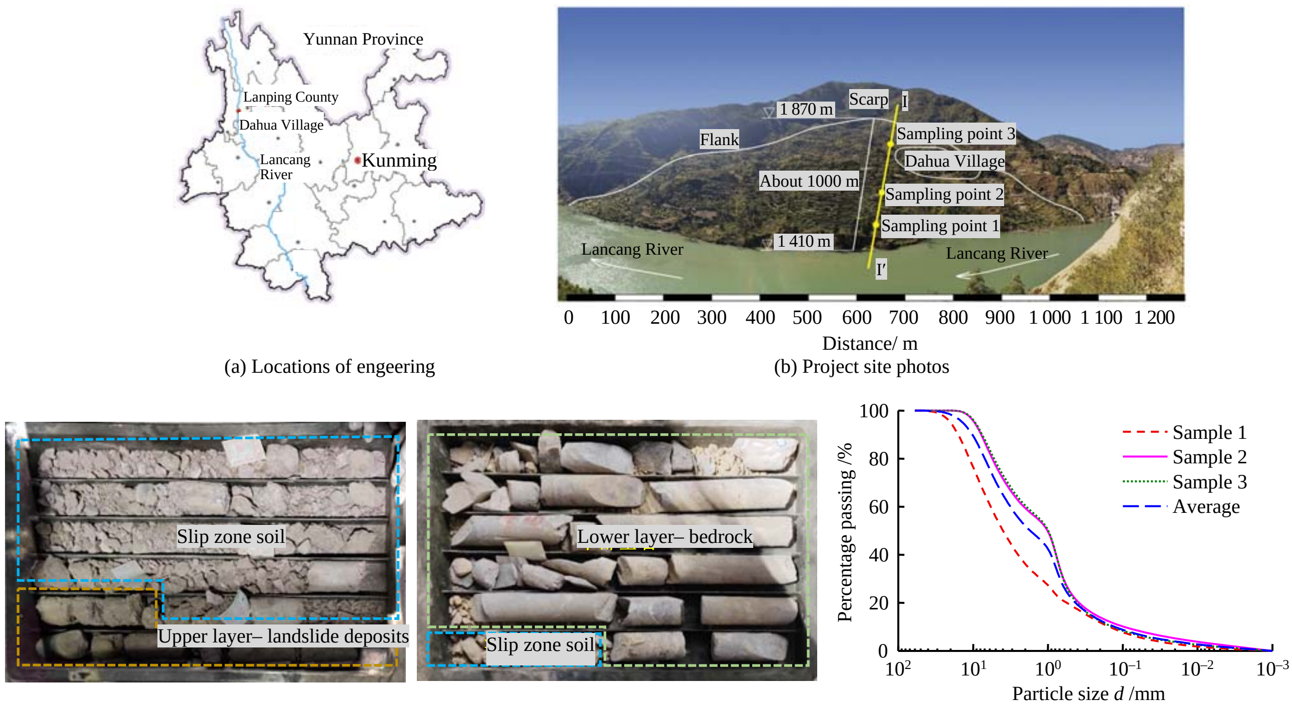

(a) Locations of engeering

(b) Project site photos

(c) Photos of borehole of slip zone soil samples

(d) Grading curves of slip zone soil samples

Fig. 1 Engineering overview of Dahua landslide deposits

The Dahua landslide deposits is about 5.1 km away from the dam site of the hydropower station. Its elevation range is 1 410–1 870 m; the length from scarp to toe is about 1 000 m, and the width along the river is about 1 060 m. The surrounding of the landslide deposits is the steep bedrock wall, which presents a shape of ‘circle chair’, forming a situation that the rear edge and side edges are surrounded by the steep bedrock while the front edge is free. The volume of the landslide is about 48 million m^3, which belongs to a large-scale landslide (Fig. 1 (b)). The main composition of the landslide deposits is as follows: (a) The accumulation body of the surface layer formed by the comprehensive action of alluvial and proluvial deposits, colluvial slope deposits and the early upper landslide, contains a lot of debris, with a loose structure, strong permeability, and a thickness of about 10–50 m. (b) The existing slip zone under the accumulation body. According to the different elevations, the buried depth is about 40–80 m, and the thickness is about 1–3 m. The specific gravity of the slip zone soil is 2.65, and the initial dry density is 1.786 g/cm^3. Observed from the sample of the slip zone soil that is exposed by the field drilling (Fig. 1 (c)), its structure is relatively loose, and part of the soil and rock are well cemented. The rock content of the slip zone soil is evidently lower than that of the accumulation body of the surface layer, but still higher than that in general landslide deposits. According to the results of sieve test on this slip zone soil, the characteristic parameters of particles were obtained as follows: the relative particle size $d_{60} = 2.29$ mm, the effective particle size $d_{10} = 0.14$ mm, the median particle size $d_{30} = 0.40$ mm, the mean particle size is 0.88 mm, the curvature coefficient $C_c = 0.51$, and the uniformity coefficient $C_u = 16.71$ (Fig.1 (d)). The lower layer of bedrock is the purplish red slate of Jurassic Bazhulu Formation (J_3b), with a relatively high strength.

Quaternary pore water is mainly distributed in the landslide deposits. The groundwater level varies with the rise and fall of the water level in gullies and river, which is mainly supplied by atmospheric precipitation and groundwater from both banks, and generally rises with the elevation of the terrain. On the whole, the groundwater in the landslide deposits is not abundant, and the water level is generally low. The monitoring data show that the Dahua landslide tends to slide along the existing sliding surface under the action of hydrodynamic factors such as rainfall and fluctuation of reservoir water level, indicating that the hydrodynamic factors have a great influence on the slip zone soil and further affect the stability of the landslide deposits.

3 Analysis of the SWCC test of slip zone soil

The slip zone soil studied in the tests is the borehole sample taken from the Dahua landslide, and the sampling location is shown in Fig. 1(b). The SWCC characteristics of slip zone soil is an important basis for studying hydrodynamic landslide. Commonly used methods for measuring SWCC include pressure plate method, tensiometer method and filter paper method[19], among which the pressure plate method is widely used because of its simplicity and ease of use.

3.1 Testing apparatus and procedures

The tests were conducted by Geo-experts high-type pressure plate apparatus for stress-dependent SWCC (SDSWCC-H), as shown in Fig.2. The apparatus is mainly composed of pressure chamber, loading device and measuring device. The main test procedures are as follows: the sample was placed on the ceramic plate with a high air entry value (AEV) in the pressure chamber, and the loading device was used to apply a constant pressure so that the sample continuously discharges water. The water was measured every 24 hours by the measuring device. When the change of water discharge within 24 hours was less than 0.1 mL for three consecutive times, it was considered that the water discharge remained constant [20]. At this time, the suction of the soil and the pressure in chamber reached equilibrium, that is, the soil–water equilibrium state. This pressure value was exactly the matric suction at this water content. The actual control range of matric suction in the test depended on the AEV of the ceramic plate. Reasonable select from the AEV of ceramic plate can not only ensure the test accuracy, but also shorten the test period[21].

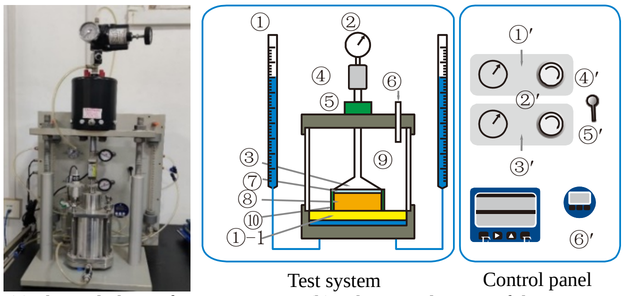

(a) Physical photo of test apparatus (b) Schematic diagram of the apparatus

①–Measuring cylinder ②–Piezometer ③–Loading cap ④–Loading disk ⑤–O-ring ⑥–Air entrance ⑦–Permeable stone ⑧–Sample ⑨–Pressure chamber ⑩–Cut ring ①–1–Ceramic plate

①′–High pressure meter and valve ②′–Transfer switch ③′–Low pressure meter and valve ④′–High pressure ⑤′–Low pressure ⑥′–Screen

Fig. 2 Photo and schematic diagrams of pressure plate apparatus

According to the characteristics of testing material and the requirements of test efficiency, the tests were carried out with the ceramic plate with an air entry value of 0.5 MPa. The maximum pressure controlled in the test was 450 kPa so as to ensure the safety of the ceramic board. The specimen in laboratory test were prepared using cutting ring, with a height of 19 mm and a diameter of 70 mm. The stress path used in the test was: 10 kPa →25 kPa→50 kPa→100 kPa→200 kPa→250 kPa→ 450 kPa.

3.1 Test results and analyses

Figure 3 shows the cumulative moisture migration under different stress levels during the test. It can be seen that in the early stage of the test, although the set pressure was only 10 kPa, the time to reach the soil–water equilibrium was relatively fast due to the high saturation, which only took about 5 days. With the increase of pressure, the moisture content in the soil continued to migrate, and the moisture content in the sample decreased, resulting in a gradual increase in the time to reach the soil–water equilibrium. In the later stage of the test, since most of the water in the sample had been discharged, the moisture content of the soil was significantly reduced, and the rate of moister migration was apparently slowed down after applying stress, thus causing the time to reach the soil–water equilibrium become longer. At the last stress level, the time to reach the soil–water equilibrium had increased to about 30 days.

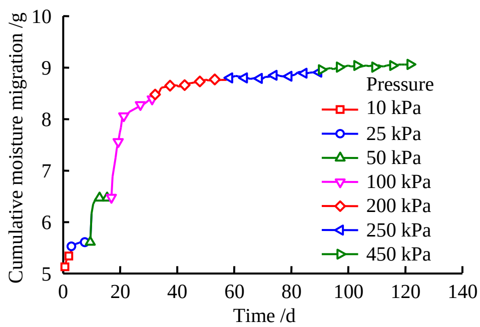

Fig. 3 Cumulative moisture migration under different pressure levels during SWCC test

According to the moisture migration at each stress level to reach the soil–water equilibrium state, the residual gravimetric water content of the sample at the current stress was calculated, and the corresponding volumetric water content can be obtained. The corresponding volume water content at each stress level was plotted in a semi-logarithmic diagram (as shown in Fig. 4), and these data points were fitted by Van Genuchten model[9], Fredlund-Xing model[22], and Brooks-Corey model[23], respectively. Results showed that the VG model could well depict the SWCC characteristics of the slip zone soil, the fitting results are shown in Fig. 4. The fitting correlation coefficient is R^2 = 0.999 998, and the formula is as follows:

$$\theta_{\mathrm{w}} = \theta_{\mathrm{r}} + \frac{(\theta_{\mathrm{s}}-\theta_{\mathrm{r}})}{\left[1+(\alpha\psi)^n\right]^{-\left(1-\frac{1}{n}\right)}} = 2.77 + \frac{(22.29-2.77)}{\left[1+(0.028\psi)^{4.30}\right]^{-0.767}} \qquad (1)$$

where θ_{w}, θ_{r}, θ_{s} are in order volumetric water content, residual water content and saturated water content(%); ψ is matric suction(kPa); α is the fitting parameter (kPa); and n is dimensionless parameter.

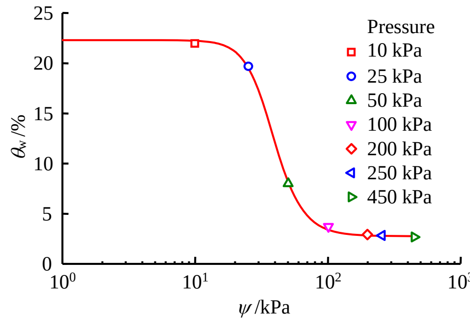

Fig. 4 Characteristic points and fitting curve of SWCC test for Dahua slip zone soil

4 Unsaturated permeability characteristics

The equation of the permeability coefficient of the unsaturated slip soil in landslide deposits can be described by matric suction head. Van Genuchten[9] proposed the formula of unsaturated permeability coefficient based on SWCC, and the formula has been widely used in the following form:

$$k = \frac{\left\{1-(\alpha h)^{n-1}\left[1+(\alpha h)^n\right]^{-\left(1-\frac{1}{n}\right)}\right\}^2}{\left[1+(\alpha h)^n\right]^{\frac{1}{2}\left(1-\frac{1}{n}\right)}} \qquad (2)$$

where k is the coefficient of permeability (cm/s); and h is the head of matric suction ψ (cm), $h = 0.1\psi$. According to the parameters of SWCC of slip soil obtained in Section 3.2, the expression of relative permeability coefficient k_{r} of slip soil is obtained by fitting as follows:

$$k_{\mathrm{r}} = \frac{\left\{1-(0.028h)^{3.30}\left[1+(0.028h)^{4.30}\right]^{-0.767}\right\}^2}{\left[1+(0.028h)^{4.30}\right]^{0.385}} \qquad (3)$$

On this basis, taking the permeability coefficient of slip soil at the time of stable seepage as the reference ($k_{\mathrm{r}} = 1.0$), the relationship between the relative permeability coefficient of slip soil k_{r} and matric suction ψ was drawn, as shown in Fig. 5.

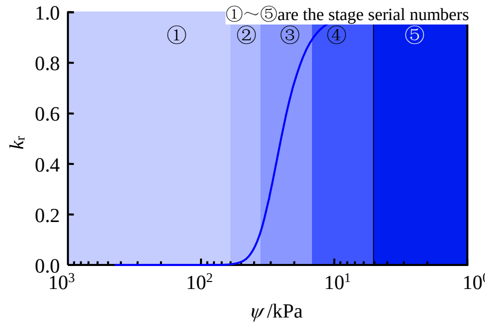

Fig. 5 Relationship between relative permeability coefficient k_r and matric suction ψ of slip soil

As can be seen from Fig. 5, with the decrease of matric suction ψ, the relative permeability coefficient of slip soil k_{r} exhibits an overall increasing tendency. According to the mutual corresponding relationship between k_{r} and ψ, the variation of the relative permeability coefficient k_{r} of slip zone soil from low to high can be roughly divided into five stages:

(1) Stage ①. The matric suction of slip zone soil began to decrease from the initial state. At this time, the relative permeability coefficient almost had no obvious change. As can be seen from the soil–water characteristic curve (Fig. 4), the water content of the sample at this time is basically residual water content in which the content of free water is very low, and the gas occupies the vast majority of pores in the soil. At this stage, water is mainly used to squeeze out the gas in the pores and occupy the pore space, so the water content will increase, and the matric suction will decrease. However, due to the difficulty of water passing through the soil, the relative permeability coefficient appears to increase slightly, which shows as an approximately horizontal line in Fig.5, and the corresponding SWCC is relatively flat.

(2) Stage ②. The slope of the curve of relative permeability coefficient begins to increase significantly. From the shape of SWCC in Fig. 4, it can be observed that the matric suction of soil decreases with the gradual increase of water content. Correspondingly, the value of matric suction at this stage drops from about 60 kPa to about 35 kPa (as shown in Fig. 5). At this stage, the gas in some pores of the slip zone soil is squeezed out and filled with free water, and some penetrating seepage channels are formed more and more quickly. Accordingly, the slope of the curve of relative permeability coefficient also increases rapidly. The formation of these penetrating seepage channels further boost the permeability of the slip zone soil. More and more water passes through the sample, showing a trend that the relative permeability coefficient increases significantly with the decrease of matric suction. This stage is shown in Fig. 5 as a concave curve.

(3) Stage ③: The relative permeability coefficient surges and approximately linearly. At this time, due to the continuous increase of water content in the slip zone soil caused by the seepage, the matric suction decreases from about 35 kPa to 15 kPa. The SWCC of slip zone soil corresponding to this stage also shows a relatively drastic change, and the shape of SWCC at this stage is nearly straight (Fig. 4). At this point, the discharge rate of pore gas is further accelerated, and more pores are occupied by water. Moreover, the seepage channels continue to grow steadily and rapidly, and the ability of water passing through the sample is enhanced rapidly. These phenomena indicate that the relative permeability coefficient increases sharply and linearly with the decrease of matric suction, corresponding to an approximate straight line in Fig. 5.

(4) Stage ④. The relative permeability coefficient increases slowly, and the slope of the curve of relative permeability coefficient decreases gradually. At this stage, the matric suction further decreases from about 15 kPa to 5.5 kPa. It can be seen from the SWCC of slip zone soil that the variation degree of the water content of slip zone soil is obviously weakened at this time (Fig. 4). As more and more gas in the pores is squeezed out, the number of new penetrating seepage channels decreases accordingly, and more and more stable seepage channels are formed by pore water. At this time, although the relative permeability coefficient still increases further, growth rate is distinctly reduced, showing an accelerated decreasing trend for the slope of the curve of relative permeability coefficient. This stage is shown in Fig. 5 as a convex curve.

(5) Stage ⑤. The relative permeability coefficient is almost stable and no longer increases. At this stage, the matric suction drops to about 5.5 kPa. As can be seen from the SWCC of slip zone soil (Fig. 4), at this time, the sample is virtually saturated, and most of the gas in the pores has been squeezed out, and the pores in the soil are almost filled with water. The seepage channels begin to stabilize and the relative permeability coefficient remain basically unchanged. This stage is shown in Fig. 5 as an approximate horizontal line.

It follows that the seepage process of unsaturated slip zone soil is closely related to the variation of matric suction, and the variation of the relative permeability coefficient of slip zone soil is consistent with the variation of the corresponding soil–water characteristic curve. This implies that the relative permeability coefficient of slip zone soil is restricted by its volumetric water content, that is, the larger the volume water content is, the greater the relative permeability coefficient is, and vice versa.

5 Experimental analysis of the saturated permeability characteristics of slip soil

When the slip soil in landslide deposits gradually transitioned from an unsaturated state to a saturated state, the water content (or matric suction) no longer change anymore, and the saturated permeability characteristics exhibited are independent of water content (or matric suction). In this section, the SLB-1 triaxial shear permeability test apparatus was used to carry out the permeability tests of the saturated Dahua slip soil under different confining pressures and different seepage pressures to study the permeability characteristics of saturated slip soil under different conditions. The dimension of the sample was 40 mm×80 mm.

5.1 Testing program

The terminal computer controller of the test system was first started. Before the test, the sample was exerted to the set confining pressure at a rate of 10 kPa/min, and then it was allowed to stand for 20 min to keep the confining pressure stable, which was used for simulating the stress state of the sample in the real environment. Then, the sample was saturated by the following steps: the head pressure of 5 kPa was applied on the bottom of the sample (upstream) until a stable water flow without air bubbles was generated at the top of the sample (downstream). At this time, the sample was considered to be saturated. After that, the osmotic pressure was loaded to the set value at a rate of 5 kPa/min upstream to simulate the permeability characteristics of the soil in the sliding zone with different hydrodynamic factors. In order to minimize the interference of other factors, the axial load was not set during the test, and the downstream of the sample was connected with the atmosphere. The test scheme is listed in Table 1. The servo system automatically recorded the amount of water discharged during the test, which was the seepage discharge. When the time for the seepage discharge to remain stable reached more than 30 minutes, the seepage flow was considered to reach a stable state at this time.

Table 1 Scheme of permeability test for slip soil

Confining pressure /kPa	Osmotic pressure /kPa
100	25，50，75
200	25，50，75，100，125，150，175
300	25，50，75，100，125，150，175，200，225，250，275

According to the results of permeability tests of slip zone soil, the variation of seepage discharge over time under different osmotic pressures and confining pressures is plotted, as shown in Fig. 6.

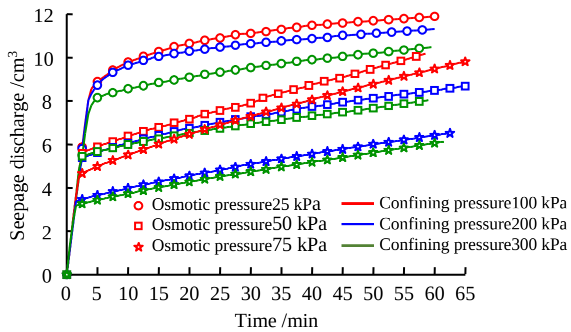

Fig. 6 Variation of the seepage discharge of slip soil over time under different seepage and confining pressures

5.2 Analysis of the variation of seepage discharge under different confining and osmotic pressures

It can be seen from Fig. 6 that when the confining pressure is the same and the osmotic pressure is different, within 2.5 minutes at the initial stage of the test, the slopes of seepage discharge curve with time are basically the same, that is, the seepage velocities are approximate, which indicates that the osmotic pressure has no obvious effect on the permeability of the sample at the initial stage of the test. With the increase of test time, the effect of osmotic pressure on permeability is gradually significant, showing that the greater the osmotic pressure is, the faster the seepage velocity is, and the shorter the time for the seepage discharge to reach a stable state is. This is mainly due to the increase of hydraulic gradient in the seepage process caused by the increase of osmotic pressure, which accelerates the process of water passing through the soil sample. It shows that the slope of the curve of stable seepage discharge with time becomes larger, that is, the seepage velocity increases with the increase of osmotic pressure.

The above phenomenons are more obvious under low confining pressure, while the difference is small under high confining pressure. This is mainly because the compactness of the soil sample is generally low under low confining pressure. With the increase of osmotic pressure, the effect of hydraulic gradient on the seepage channel becomes greater. When the confining pressure becomes higher, the structure of the soil sample is com- pressed, the porosity of the soil sample decreased, and the ability of water to pass through the soil is weakened, resulting in the weakening of the difference of seepage velocity.

5.3 Analysis of seepage flow under same osmotic pressure and different confining pressures

When the osmotic pressure is the same, the lower the confining pressure is, the greater the permeability of the sample is. On the contrary, the higher the confining pressure is, the smaller the permeability of the sample is. At the initial stage of the test, the curves under different confining pressures almost overlap, which shows that the seepage velocities are basically the same under different confining pressures. With the gradual increase of time, the performance of seepage discharge begins to differentiate, and the seepage dis- charge increases approximately linearly with time, after which the seepage velocity gradually reaches a stable value.

Under the same osmotic pressure, with the increase of confining pressure, the seepage discharge increases nonlinearly, and the increase is gradually smaller. This is mainly due to the fact that the porosity of the sample does not change much at a low confining pressure. However, the sample has a certain degree of shrinkage deformation at a higher confining pressure, leading to a reduction in porosity. Thus, some seepage channels in the sample are blocked, then the seepage paths are enlarged, which makes it more difficult for water to pass through the sample the seepage discharge declines. With the further increase of confining pressure, since the sample has been compressed to a certain extent, the further decrease of the porosity of soil sample is limited, and the reduction of seepage channel is lower than before.

5.4 Analysis of saturated seepage flow under different confining pressures

The hydraulic gradient J is plotted in Fig. 7 with respective steady seepage velocity v of slip zone soil samples under different confining pressures. It can be observed that the curve shows an obvious nonlinear relationship under different confining pressures, indicating that the permeability characteristics of soil samples in the sliding zone do not satisfy the linear Darcy's law.

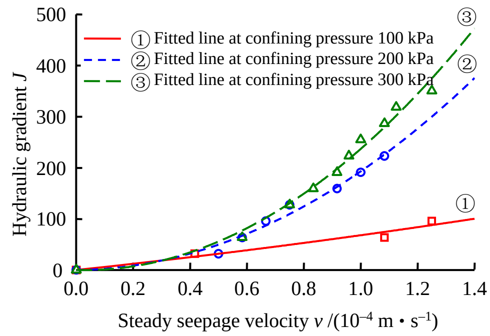

Fig. 7 Relationships between *J* and *v* under different confining pressures

From Fig.7, it can be seen that the nonlinear relationship between hydraulic gradient and seepage velocity became stronger as the confining pressure increase. Hence, the Forchheimer binomial function $J = av + bv^2$ (where a and b are the coefficients of the first and second terms, respectively) was used to fit the relationship between the seepage velocity and hydraulic gradient of slip soil with different confining pressures, and the following expression was obtained:

$$J=\begin{cases}59.08v+9.088v^2 & \text{(Confining pressure100 kPa)}\\ 5.583v+187.5v^2 & \text{(Confining pressure200 kPa)}\\ 237.8v^2 & \text{(Confining pressure300 kPa)}\end{cases} \tag{4}$$

where $a = 59.08$ and $b = 9.088$, and the correlation coefficient $R^2 = 0.98532$ when the confining pressure is 100 kPa; $a = 5.583$ and $b = 187.5$, and the correlation coefficient $R^2 = 0.99478$ when the confining pressure is 200 kPa; $a \approx 0$ and $b = 237.8$, and the correlation coefficient $R^2 = 0.99697$ when the confining pressure is 300 kPa. The results show that the Forchheimer binomial function has a better fitting effect.

Based on Eq. (4), the flow regime in the process of seepage of saturated slip soil under different confining pressures is affected by both the first term, $J_1 = av$, and the second term, $J_2 = bv^2$, of seepage velocity, where $J_1 = av$ can be expressed as $v = AJ_1$ $(A = 1/a)$, and it represents linear flow; $J_2 = bv^2$ can expressed as $v = BJ_2^{\frac{1}{2}}$ $(B = \sqrt{1/b})$, and it represents nonlinear flow. When the confining pressure gradually increases from 100 kPa to 300 kPa, the effect of the first term of seepage velocity (linear flow) on the hydraulic gradient decreases gradually, whilst the effect of the second term of seepage velocity (nonlinear flow) on the hydraulic gradient increases gradually. When the confining pressure is 300 kPa, the coefficient of the first term of seepage velocity a is approximately 0, and the value of b continues to increase to 237.8. At this time, the hydraulic gradient is only related to the second term of seepage velocity. According to the above results, Fig. 8 shows the relationship between the coefficients of seepage velocity a , b and confining pressure.

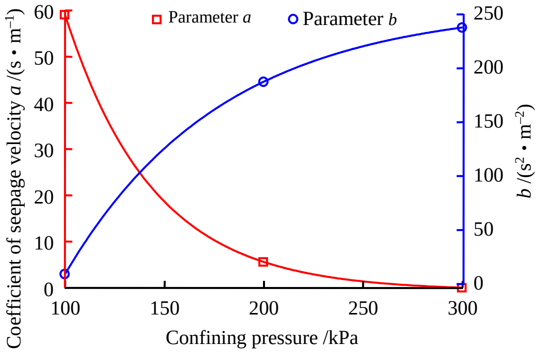

Fig. 8 Scatter plots of parameter values of *a* and *b* under different confining pressures

It can be seen from Fig. 8 that with the increase of confining pressure, a keeps decreasing and b keeps increasing. The main reason for this phenomenon is that the soil and rock in slip soil are interlaced and overlapped with each other. When the confining pressure is low, the soil sample is almost not compressed and remains in the original state. At this time, the compactness of the soil sample is generally poor, and a large number of pores in the soil sample are interconnected to form a relatively complete seepage channel. The water flow in these pores shows a linear relationship. In addition, at a large number of soil-rock interfaces that exist in slip zone soil, water flow is mainly manifested by the flow of water around the edge of the rock block. This water flow around the edge of the rock block shows a nonlinear flow regime When the compactness of the soil sample is not high, the linear flow along the pores is dominant, and the nonlinear flow along the interface is auxiliary, showing that the coefficient a is relatively larger and the coefficient b is relatively smaller. When the confining pressure begins to increase, the compactness of soil sample increases, and part of the seepage channels are blocked. The large- scale pores are further compressed into small-scale pores, and the number of penetrating seepage channels is greatly reduced, which shows that the effect of linear flow decreases significantly, and the value of a decreases rapidly. At this time, the proportion of the water flow at the soil-rock interface increases greatly, showing that the effect of nonlinear flow is more significant, and the value of b rises sharply. When the confining pressure increases further, the soil sample is compressed continuously. At this point, the large pores have been basically compressed into small pores, and the penetrating phenomenon between the pores almost disappears, showing that the effect of linear flow is reduced to the minimum, and the value of a gradually decreases and even tends to zero. However, the water flow along the soil–rock interface becomes absolutely dominant, and the value of b further increases. The flow regime in the process of seepage of saturated slip soil is mainly a completely nonlinear flow pattern. As the soil sample is compressed greatly in the process of increasing stable confining pressure in the early stage, the coefficients a and b decrease (rises) at a faster rate. At the later stage of the test, it is more difficult for soil samples to be compressed, in which the change in seepage channel is weakened, and the change rates of coefficients a and b are obviously reduced.

6 Conclusions

In this paper, the landslide deposit of Dahua landslide in Dahuaqiao Hydropower Station was selected as the research object, and the soil–water characteristic curve of the slip zone soil in landslide deposits was measured in laboratory test. On this basis, the permeability characteristics of the unsaturated slip zone soil were obtained through further analysis. A series of permeability tests under different confining pressures and osmotic pressures was also carried out. The unsaturated and saturated permeability characteristics of the slip soil in landslide deposits were obtained, which provides reference and basis for analyzing the failure mechanism of hydrodynamic landslide with deposits. The main conclusions are therefore derived from this work:

(1) The VG model can be used to well describe the soil–water characteristic curve and unsaturated permeability of the slip zone soil in Dahua landslide deposits. The variation of the relative permeability coefficient of slip zone soil is consistent with the variation of the matric suction of slip zone soil. The change of the relative permeability coefficient is restricted by the volumetric water content, that is, the larger the volumetric water content is, the greater the relative permeability coefficient is, and vice versa. The whole change process of relative permeability coefficient can be roughly divided into five different stages: slight increase, significant increase, sharp increase, slow increase, and stable state.

(2) When the slip zone soil is in a saturated permeability state, under the same confining pressure, the greater the osmotic pressure, the greater the influence of the increasing hydraulic gradient on the seepage channel, indicating the permeability of soil is stronger. This phenomenon becomes more significant under low confining pressure. Under the same osmotic pressure, the lower the confining pressure is, the stronger the permeability is; and with the increase of confining pressure, the permeability of slip zone soil decreases. This is mainly because when the confining pressure is high, the soil structure is compressed, and the porosity is reduced, so the ability of water to pass through the soil sample is weakened.

(3) The relationship between seepage velocity and hydraulic gradient of saturated slip zone soil shows strong non-Darcy flow characteristics. The permeability characteristic of saturated slip zone soil conforms to

the Forchheimer binomial function $J = av + bv^2$, that is, it is controlled by the dual actions of linear flow and nonlinear flow. In the Forchheimer binomial function, the coefficients a and b decrease and increase, respectively, with the increase of confining pressure. In the initial several stages of increasing confining pressure, the changes in coefficients a and b are more significant. As the confining pressure further increases, the changes in coefficients a and b obviously weaken. When the confining pressure increases to a certain value, the permeability characteristic of saturated slip soil is mainly dominated by the second term of seepage velocity.

References

[1] KEEFER D K, WILSON R C, MARK R K, et al. Real-time landslide warning during heavy rainfall[J]. Science, 1987, 238(4829): 921–925.

[2] ZHOU Jia-wen, XU Wei-ya, DENG Jun-ye, et al. Stability analysis of slope under the condition of rainfall infiltration[J]. Journal of Hydraulic Engineering, 2008, 39(9): 1066–1073.

[3] GUO Zhi-hua, ZHOU Chuang-bing, SHENG Qian, et al. Influence of reservoir water level variation on slope stability[J]. Rock and Soil Mechanics, 2005, 26(Suppl.2): 29–32.

[4] ZHOU Jia-wen, CHEN Ming-liang, LI Hai-bo, et al. Formation and movement mechanisms of water-induced landslides and hazard prevention and mitigation techologies[J]. Journal of Engineering Geology, 2019, 27(5): 1131–1145.

[5] JIANG Qiang-qiang, JIAO Yu-yong, SONG Liang, et al. Experimental study on reservoir landslide under rainfall and water-level fluctuation[J]. Rock and Soil Mechanics, 2019, 40(11): 4361–4370.

[6] WANG Si-jing, MA Feng-shan, DU Yong-lian. On the rock-water interaction in reservoir areas and its geo-environmental effect[J]. Journal of Engineering Geology, 1996, 4(3): 1–9.

[7] XU Wen-jie, CHEN Zu-yu, HE Bing-shun, et al. Research on river-blocking mechanism of Xiaojiaqiao landslide and disasters of chain effects[J]. Chinese Journal of Rock Mechanics and Engineering, 2010, 29(5): 933–942.

[8] ALAOUI A, LIPIEC J, GERKE H H. A review of the changes in the soil pore system due to soil deformation: a hydrodynamic perspective[J]. Soil and Tillage Research, 2011, 115-116: 1–15.

[9] VAN GENUCHTEN M T. A closed-form equation for predicting the hydraulic conductivity of unsaturated soils[J]. Soil Science Society of American Journal, 1980, 44(5): 892–898.

[10] FREDLUND D G, XING A Q, HUANG S Y, e. al. Predicting the permeability function for unsaturated soils using the soil-water characteristic curve[J]. Canadian Geotechnical Journal, 1994, 31(4): 533–546.

[11] WANG Shi-mei, LIU De-fu, TAN Yun-zhi, et al. Experimental research on soil-water characteristic curves of soils for a landslide[J]. Rock and Soil Mechanics, 2008, 29(10): 2651–2654.

[12] PHAM K, LEE H, KIM D, et al. Influence of hydraulic characteristics on stability of unsaturated slope under transient seepage conditions[J]. Landslides, 2018, 15(9): 1787–1799.

[13] YU Xiao-jun, MA Qing-hai, YANG Tian-hong, et al. Study on influence to seepage state and non-Darcy seepage parameters by graduation characteristics of fault material[J]. Site Investigation Science and Technology, 2018, 219(5): 15–21.

[14] WHITAKER S. The Forchheimer equation: a theoretical development[J]. Transport in Porous Media, 1996, 25(1): 27–61.

[15] ZHOU Z, YANG H, WANG X, et al. Model development and experimental verification for permeability coefficient of soil-rock mixture[J]. International Journal of Geomechanics, 2017, 17(4): 1–10.

[16] ZHOU Zhong, FU He-lin, LIU Bao-chen, et al. Experimental study of the permeability of soil-rock-mixture[J]. Journal of Hunan University (Natural Sciences), 2006, 33(6): 25–28.

[17] SHEN Hui, LUO Xian-qi, BI Jin-feng. Numerical simulation of internal erosion characteristics of block in matrix soil aggregate[J]. Rock and Soil Mechanics, 2017, 38(5): 1497–1502.

[18] ZHONG Zu-liang, BIE Cong-ying, HU Lun, et al. Research on one-dimensional consolidation model of soil-rock mixtures backfill under Forchheimer seepage mode[J]. Chinese Journal of Underground Space and Engineering, 2019, 15(2): 473–488.

[19] LU N, LIKOS W J. Unsaturated soil mechanics[M]. New Jersey: Wiley, 2005.

[20] FREDLUND D G, PHAM H Q. A Volume-mass constitutive model for unsaturated soils in terms of two independent stress state variables[C]//4th International Conference on Unsaturated Soils. Carefree: [s. n.], 2006: 105–134.

[21] LIU Feng-yin, ZHANG Zhao, ZHOU Dong, et al. Debugging of GCTS-Type SWCC device and analysis of the corresponding technical indexes[J]. Journal of Xi'an University of Technology, 2010, 26(3): 320–325.

[22] FREDLUND D G, XING A. Equations for the soil-water characteristic curve[J]. Canadian Geotechnical Journal, 1994, 31(4): 521–532.

[23] BOOKS R, COREY A. Hydraulic properties of porous media and their relation to drainage design[J]. Transactions of the ASAE, 1964, 24(7): 26–28.